Criticality triggers the emergence of collective intelligence in groups

Ilario De Vincenzo,[1] Ilaria Giannoccaro,[1] Giuseppe Carbone,[1,2,3] and Paolo Grigolini[4]

[1]*Department of Mechanics, Mathematics and Management, Politecnico di Bari, v.le Japigia 182, 70126 Bari, Italy*

[2]*Physics Department M. Merlin, CNR Institute for Photonics and Nanotechnologies U.O.S. Bari via Amendola 173, 70126 Bari, Italy*

[3]*Department of Mechanical Engineering, Imperial College London, London, South Kensington Campus, London SW7 2AZ, United Kingdom*

[4]*Center for Nonlinear Science, University of North Texas, P.O. Box 311427, Denton, Texas 76203-1427, USA*

(Received 15 March 2017; revised manuscript received 5 July 2017; published 11 August 2017)

A spinlike model mimicking human behavior in groups is employed to investigate the dynamics of the decision-making process. Within the model, the temporal evolution of the state of systems is governed by a time-continuous Markov chain. The transition rates of the resulting master equation are defined in terms of the change of interaction energy between the neighboring agents (change of the level of conflict) and the change of a locally defined agent fitness. Three control parameters can be identified: (i) the social interaction strength βJ measured in units of social temperature, (ii) the level of confidence β' that each individual has on his own expertise, and (iii) the level of knowledge p that identifies the expertise of each member. Based on these three parameters, the phase diagrams of the system show that a critical transition front exists where a sharp and concurrent change in fitness and consensus takes place. We show that at the critical front, the information leakage from the fitness landscape to the agents is maximized. This event triggers the emergence of the collective intelligence of the group, and in the end it leads to a dramatic improvement in the decision-making performance of the group. The effect of size M of the system is also investigated, showing that, depending on the value of the control parameters, increasing M may be either beneficial or detrimental.

DOI: 10.1103/PhysRevE.96.022309

I. INTRODUCTION

Human groups are proven to outperform single individuals in solving a variety of complex tasks in many different fields, including new product development, organizational design, strategy planning, research and development. Their superior ability originates from the collective decision making: individuals make choices, pursuing their individual goals on the basis of their own knowledge or expertise and adapting their behavior to the actions of the other agents. Social interactions, indeed, promote a mechanism of consensus-seeking within the group, but they also provide a useful tool for knowledge and information-sharing [1–5]. This type of decision-making dynamics is common to many social systems in nature, e.g., flocks of birds, herds of animals, ant colonies, schools of fish [3,6–15], as well as bacterial colonies [16–18], and even artificial systems [19–22].

Even though the single agent possesses limited knowledge, and the actions it performs are usually very simple, the collective behavior leads to the emergence of a superior intelligence known as swarm or collective intelligence [23–26], which has recently been receiving a growing amount of attention in the literature with regard to its antecedents and proper measures [27,28]. In the past few years, a great deal of research has been aimed at improving our knowledge of social behavior in natural systems [29–31], with the goal of understanding the physical origin of the collective intelligence of such systems [1,32–36]. A large part of those studies recognized consensus-seeking as one of the key factors in the decision-making process, enabling the emergence of collective intelligence [37–45]. However, it was also recognized that the development of brand new technologies, products, and novel findings may be the result of accidental events or the outcome of extremely gifted minds, as in the case of scientific discoveries leading to Nobel prizes being awarded. Therefore, in modeling the decision-making process of human groups, one has to take into account the effect of social interactions, which promote consensus-seeking, but also the influence of the level of expertise or knowledge of individuals. From this perspective, a few models of decision-making can be found in the literature. Those models attempt to capture the influence of the main drivers of the individual behavior in groups, and in particular of self-interest and consensus-seeking [46–50]. Following this line of research, in this paper we employ a model of decision-making, already proposed in [50], in which consensus-seeking is modeled using the Ising-Glauber dynamics [51,52], whereas the knowledge of each member in the group is modeled through an individual fitness landscape described in terms of a Kauffman NK model [53,54]. A continuous-time Markov chain governs the decision-making process, where the transition rates of an individual's change of opinion are represented by the product of the Ising-Glauber rate [52,55–58], which mimics the process of consensus-seeking within the group, and the Weidlich exponential rate [59,60], which speeds up or slows down the change of opinion depending on the level of individual fitness. Here, we explore how the dynamics of the system is affected by the strength of social interactions, the level of knowledge of individuals, and their self-confidence. In particular, we focus on the behavior of the system at criticality, where a phase transition and a significant amount of information exchange occur, and we study how these conditions are related to the emergence of collective intelligence of the group. Recent investigations suggest that criticality and large amounts of information flow are the conditions leading to the emergence of collective intelligence [25,63–72].

II. THE DECISION-MAKING MODEL

Here we summarize the decision-making model (DMM) proposed by two of the authors in Ref. [50]. We consider a

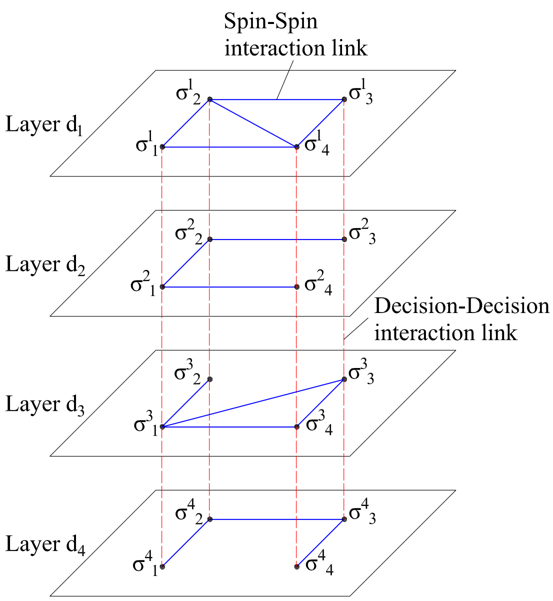

FIG. 1. The multiplex network utilized to build up the model. Observe that on each decision layer the structure of the social network (blue links) may be different. Blue links identify those spins (on a given layer) that interact through an Ising-like interaction energy. Red dashed links connect the different decision layers. These types of links identify, for any given member, the interaction among spins on the different decision layer, leading to an additional energy term that provides the fitness of each single member of the group.

set of M interacting agents, which is assigned to carry out a task. The latter consists in attempting to solve a complex combinatorial problem by identifying the set of configurations with the highest fitness of the group, out of a certain finite (but large) number of different configurations.

A. The Hamiltonian of the system

Consider a discrete system comprised of M agents. Each agent is characterized by a state vector $\boldsymbol{\sigma}_k = (\sigma_k^1,\sigma_k^2,\dots,\sigma_k^N)$, $k = 1,2,\dots,M$. The spin $\sigma_k^j = \pm 1$, $j = 1,2,\dots,N$, is a binary variable taking only two possible values ± 1. It represents the opinion that the agent k has on the jth decision variable d_j. Each decision variable identifies a "decision layer" (see Fig. 1), where spin-spin interactions occur leading to the definition of an Ising-like energy term.

The entire system is then described by a multiplex network. Moreover, interaction among the different decision layers occurs as a consequence of the fact that each state vector $\boldsymbol{\sigma}_k$ is associated with a certain energy level that defines the fitness of the k-agent. The Hamiltonian of the system is then

$$H(\mathbf{s}) = E(\mathbf{s}) - \rho V(\mathbf{s}) = -\frac{1}{2} J \mathbf{A}\mathbf{s}\cdot\mathbf{s} - \rho V(\mathbf{s}) = -\frac{1}{2} J \sum_{ij} A_{ij} s_i s_j - \rho V(\mathbf{s}), \tag{1}$$

where the state vector $\mathbf{s}$ of the whole system is a vector of $n = M \times N$ components $\mathbf{s} = (\mathbf{s}_1,\mathbf{s}_2,\dots,\mathbf{s}_M) = (\sigma_1^1,\sigma_1^2,\dots,\sigma_1^N,\sigma_2^1,\sigma_2^2,\dots,\sigma_2^N,\dots,\sigma_M^1,\sigma_M^2,\dots,\sigma_M^N)$, $E(\mathbf{s})$ is the Ising energy, due to the mutual spin-spin interaction, and $V(\mathbf{s})$ is the fitness associated with the state vector $\mathbf{s}$. In Eq. (1), A_{ij} are the elements of an N-block adjacency matrix $\mathbf{A}$. Note that $\mathbf{A}$ is a block matrix, since social interactions occur only among the spin belonging to the same decision layer. The independent parameter ρ defines the weight of the fitness $V(\mathbf{s})$ compared to the Ising energy $E(\mathbf{s})$.

B. The Markov chain formulation

Starting from any initial condition, the dynamics of the system of spins, identified by the Hamiltonian Eq. (1), can be modeled in terms of a continuous-time Markov chain where the probability $P(\mathbf{s},t)$ that at time t the state vector takes the value $\mathbf{s}$ out of $2^{M\times N}$ possible states satisfies the master equation

$$\frac{dP(\mathbf{s},t)}{dt} = -\sum_l w(\mathbf{s}_l \to \mathbf{s}_l')P(\mathbf{s}_l,t) + \sum_l w(\mathbf{s}_l' \to \mathbf{s}_l)P(\mathbf{s}_l',t), \tag{2}$$

where $\mathbf{s}_l = (s_1,s_2,\dots,s_l,\dots,s_n)$ and $\mathbf{s}_l' = (s_1,s_2,\dots,-s_l,\dots,s_n)$. The transition rate of the Markov chain (i.e., the probability per unit time that the opinion s_l flips to $-s_l$ while the others remain temporarily fixed) is chosen by following a similar argument to that presented by Glauber [52], and it is the product of an Ising-like term that models the process of consensus-seeking aimed at minimizing the level of social conflict, and the Weidlich exponential rate [59,60], which models the self-interest behavior of the agents, i.e.,

$$w(\mathbf{s}_l \to \mathbf{s}_l') = \frac{1}{2}\left[1 - s_l \tanh\left(\frac{\beta J}{\langle\kappa\rangle}\sum_h A_{lh}s_h\right)\right] \times \exp\{\beta'[\Delta V(\mathbf{s}_l',\mathbf{s}_l)]\}. \tag{3}$$

In Eq. (3), A_{lh} are the elements of the N-block adjacency matrix $\mathbf{A}$. The quantity βJ can be interpreted as the social interaction strength measured in units of temperature β^{-1}, and $\langle\kappa\rangle$ is the mean degree of the network of interactions among the agents on each decision layer. The use of the reduced coupling constant $J/\langle\kappa\rangle$ is needed to guarantee that independent of the type of network structure, the Ising energy term is an extensive physical quantity. In fact, for the case of a fully connected network, such as the one considered in this study, the quantity $\langle\kappa\rangle = M - 1$ and the number of links among the nodes is $M(M-1)/2$. Hence, the term $\sum_{ij} A_{ij}s_is_j$ in Eq. (1) increases quadratically with M, but dividing by $\langle\kappa\rangle$ would again lead the Ising-like interaction energy to increase linearly with the number of nodes M. The quantity β can be interpreted as the degree of trust the members have in the judgement or opinion of others. Similarly, the quantity $\beta' = \beta\rho/2$ can be related to the level of confidence the members have about their perceived fitness, i.e., about their own knowledge or expertise. Note that the Markov process Eq. (2) with transition rates Eq. (3) is shown to obey the detailed balance conditions (see Ref. [50]), with steady-state probability $P(\mathbf{s},t \to +\infty) = P_0(\mathbf{s}) = \mathcal{Z}^{-1}\exp[-\beta E(\mathbf{s}) + 2\beta' V(\mathbf{s})]$, where the partition function $\mathcal{Z} = \sum_{\mathbf{s}} \exp[-\beta E(\mathbf{s}) + 2\beta' V(\mathbf{s})]$. The quantity

$\Delta V(\mathbf{s}'_l,\mathbf{s}_l)$ is simply the change of fitness of the agent when its opinion changes from s_l to $-s_l$.

C. Group decision and the degree of consensus

As the process evolves, the bit-string $\mathbf{d}(t)$ of the decision of the group of agents needs to be determined at each time step t given the state vector $\mathbf{s}(t)$. Different choices can be made. Among these, the majority rule seems appropriate, especially in the presence of cognitive limits of the agents, as it avoids the need for inquiring about the value of fitness perceived by each agent at time t. Therefore, given the set of opinions $(\sigma_1^j,\sigma_2^j,\ldots,\sigma_M^j)$ that the agents have about the decision j, at time t, we set

$$d_j(t) = \mathrm{sgn}\left[M^{-1}\sum_k \sigma_k^j(t)\right], \quad j = 1,2,\ldots,N. \tag{4}$$

If M is even and in the case of a parity condition, d_j is uniformly chosen at random between the two possible values ± 1. The group fitness is then calculated as $V(t) = V[\mathbf{d}(t)]$ and the ensemble average $\langle V(t)\rangle$ is then evaluated together with the degree of consensus among the agents [50],

$$\chi(t) = \frac{1}{M^2 N}\sum_{j=1}^{N}\sum_{kh=1}^{M} R_{hk}^j(t), \tag{5}$$

where $R_{hk}^j(t) = \langle \sigma_k^j(t)\sigma_h^j(t)\rangle$. Observe that $0 \leqslant \chi(t) \leqslant 1$.

III. THE FITNESS LANDSCAPE

In this section, we define the complex fitness landscape of the system. More precisely, the fitness landscape is defined consisting of 2^N discrete values. To identify each single value, we first need to label each of them, in other words we need to count them. Toward that end, we use a binary numeral system so that each fitness value is identified by a bit-string $\mathbf{d} = (d_1,d_2,\ldots,d_N)$, where each variable $d_i = \pm 1$, $i = 1,2,\ldots,N$ is a two-state variable. The total number of different configurations is 2^N, and each bit-string $\mathbf{d}$ is then associated with a certain fitness value $V(\mathbf{d})$. The discrete landscape $V(\mathbf{d})$ may be almost anything, e.g., it may be represented by the length of the Hamiltonian cycle in the traveling salesman problem (TSP) [73], the optimization function in the knapsack problem [74], the Kauffman NK landscape [53,54], a fractal landscape [75] (see also Appendix 2), or any other complex landscape [76]. In this study, we will make use of the complex landscape defined within the framework of the NK Kauffman model of combinatorial complexity [53,54]. The motivation of this choice is that within the NK framework, it is relatively easy to model the cognitive capabilities of each agent in the groups (i.e., it is easy to take into account that each agent in the group has his own personal understanding of the problem), and to tune the complexity of the landscape through the parameters N and K. Within the NK approach, the discrete fitness function $V(\mathbf{d})$ is computed as the weighted sum of N independent stochastic contributions $W_j(\mathbf{d}_j^K)$, $j = 1,2,\ldots,N$, which only depend on the corresponding sub-bit-string $\mathbf{d}_j^K = (d_j,d_j^1,\ldots,d_j^K)$ of length $K+1$, where K may take the values $K = 0,1,\ldots,N-1$ [53,54]. The number of different values that each contribution $W_j(\mathbf{d}_j^K)$ may take is 2^{K+1}, i.e., it is equal to the number of different configurations that can be enumerated with a $K+1$ bit-string. The fitness landscape of the group $V(\mathbf{d})$ is then defined as

$$V(\mathbf{d}) = \frac{1}{N}\sum_{j=1}^{N} W_j\left(\mathbf{d}_j^K\right). \tag{6}$$

The integer index K tunes the complexity of the problem: increasing K increases the complexity C. Consider, indeed, that the entire NK fitness landscape can be generated (see Appendix A) by combining together, through Eq. (6), $L = 2^{K+1}N$ different values, drawn at random from a uniform distribution. Thus, we need to specify L different numbers to completely define the NK fitness landscape. With this in mind, we can easily estimate the complexity C as

$$C = \log_2 L = K + 1 + \log_2 N. \tag{7}$$

Equation (7) shows that the parameter K is much more influential than N in affecting the complexity of the landscape. It is worth noticing that for $K = N-1$ the complexity becomes $C = N + \log_2 N$ and $L = 2^N N$, which then increases exponentially with N. Recalling that a measure of complexity is also provided by the number of local maxima, we expect that, for $K = N-1$, also the number of local optima increases exponentially with N. This has been indeed found by Kauffman [53,54], who showed that, under the condition $K = N-1$, the number of local optima is on average $2^N/(N+1)$. Incidentally, we note that solving an NK Kauffman combinatorial problem, i.e., finding the optimum of the NK landscape, is classified for $K > 2$ as an NP-complete problem [77].

In our DMM model, each agent in the group possesses a specific cognitive level (i.e., the level of knowledge). To model this level of knowledge, we introduce the probability $p \in [0,1]$ that each single agent knows the contribution $W_j(\mathbf{d}_j)$ to the total fitness. Based on its level of knowledge, each agent k can then compute its own perceived fitness as

$$V_k(\mathbf{d}) = \frac{\sum_{j=1}^{N} D_{kj} W_j\left(\mathbf{d}_j^K\right)}{\sum_{j=1}^{N} D_{kj}}, \tag{8}$$

where $\mathbf{D}$ is the matrix whose elements D_{kj} take the value 1 with probability p and 0 with probability $1-p$. Observe that when $p = 0$ all the elements $D_{kj} = 0$, at which point we set $V_k(\mathbf{d}) = 0$. Observe that with this definition of perceived fitness $V_k(\mathbf{d})$ the quantity $\Delta V(\mathbf{s}'_l,\mathbf{s}_l)$ appearing in Eq. (3) is $\Delta V(\mathbf{s}'_l,\mathbf{s}_l) = V_k(\boldsymbol{\sigma}'_k) - V_k(\boldsymbol{\sigma}_k)$, with $\boldsymbol{\sigma}_k = (\sigma_k^1,\sigma_k^2,\ldots,\sigma_k^j,\ldots,\sigma_k^N)$ and $\boldsymbol{\sigma}'_k = (\sigma_k^1,\sigma_k^2,\ldots,-\sigma_k^j,\ldots,\sigma_k^N)$, i.e., as mentioned so far, it is the change of the fitness perceived by the agent $k = \mathrm{quotient}(l-1,N)+1$ when its opinion σ_k^j on the decision $j = \mathrm{mod}(l-1,N)+1$ changes from $s_l = \sigma_k^j$ to $s'_l = -\sigma_k^j$.

IV. CRITICALITY, MUTUAL INFORMATION, AND THE EMERGENCE OF COLLECTIVE INTELLIGENCE

Calculations have been carried out assuming that the network of social interactions on each single decision layer is fully connected. We simulate the Markov process by using the well-established stochastic simulation algorithm

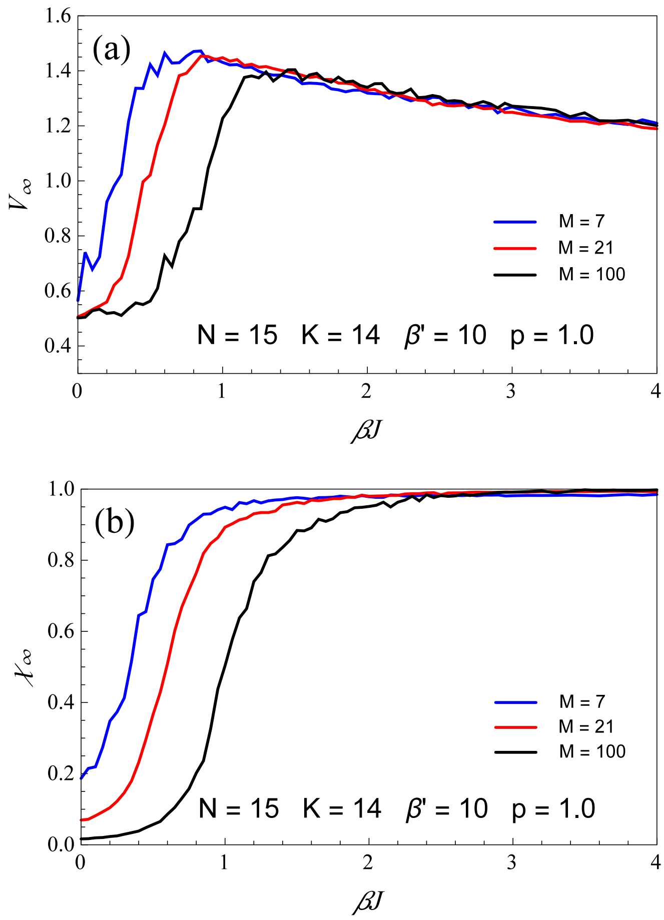

FIG. 2. The stationary values of the normalized averaged fitness V_∞ (a) and of the statistically averaged consensus χ_∞ (b) as a function of βJ. Results are presented for $\beta' = 10$, $p = 1$, $N = 15$, and $K = 14$, and for three different team sizes $M = 7, 21$, and 100.

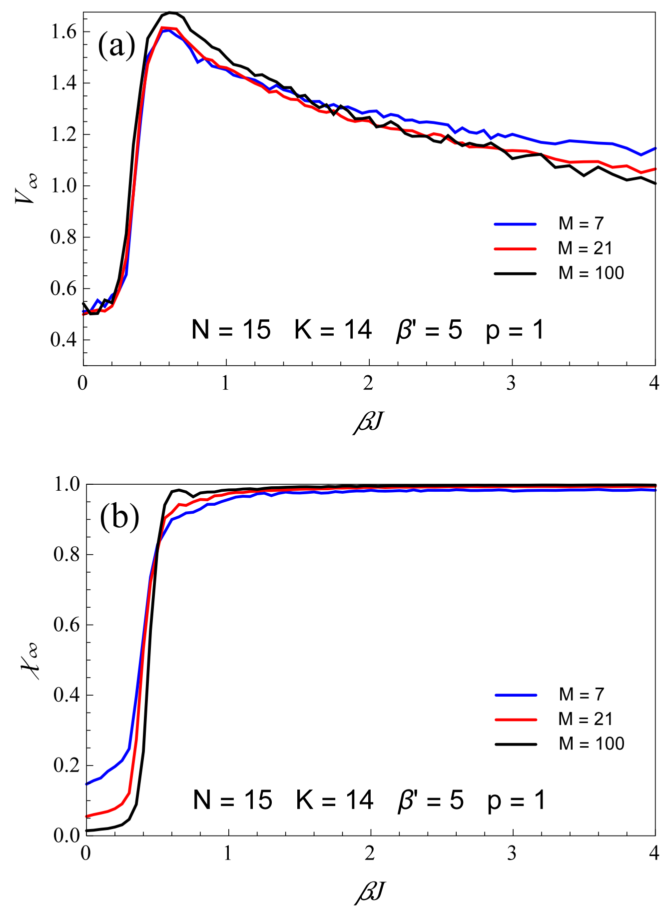

FIG. 3. The stationary values of the normalized averaged fitness V_∞ (a) and of the statistically averaged consensus χ_∞ (b) as a function of βJ. Results are presented for $\beta' = 5$, $p = 1$, $N = 15$, and $K = 14$, and for three different team sizes: $M = 7, 21$, and 100.

proposed by Gillespie [50,61,62]. For any given set of input parameters, we computed hundreds of different realizations of the same process (we replicated the simulations 200 times) and calculated the ensemble average of the realizations. The simulation stopped at steady state, i.e., when changes in the time averages of consensus and group fitness over consecutive time intervals of a given length were sufficiently small.

In Fig. 2 we show the stationary values of fitness $V_\infty = \langle V(t \to \infty)\rangle$ and the degree of consensus $\chi_\infty = \langle \chi(t \to \infty)\rangle$ as a function of the quantity βJ for different group sizes $M = 7, 21$, and 100, and $N = 15$, $K = 14$, $\beta' = 10$, and for a level of knowledge $p = 1.0$.

Results clearly show that a critical range of βJ values exists at which both consensus and fitness have a sharp and concurrent increase. Notably, this transition from low to high fitness is affected by the group size M, in that, for given $\beta' = 10$ and $p = 1.0$, an increase of M moves the transition to higher values of βJ. Somehow unexpectedly, increasing M does not seem to sharpen this transition, which occurs instead in a pure Ising system. This is clearly related to the presence of an additional energy term in the Hamiltonian of the system. Indeed, in our model, two terms contribute to the total energy of the system: (i) the Ising social interaction energy, i.e., the level of conflict (or disagreement) within the group, and (ii) the energy term associated with the perceived (individual) fitness. The latter breaks the symmetry of the system dynamics, making it sensitive to the parameter β'. Thus, for $\beta' = 5$ (the other quantities being fixed), the trend of V_∞ and χ_∞, represented in Fig. 3, differs from the case $\beta' = 10$, and, this time, it resembles closely what is expected for the pure Ising systems. Indeed, the transition is much steeper and becomes sharper and sharper as the number of agents M is increased.

To identify the presence of phase transitions and critical fronts, we represent, for given values of p and M, the long-term system response (i.e., the steady-state response), in terms of average fitness V_∞ and level of consensus χ_∞, as a function of βJ and β'. The phase diagrams can then be generated, and the critical transition fronts identified. An example is reported in Fig. 4 for $p = 1$, $N = 15$, $K = 14$, and $M = 7$. A critical transition front can be clearly observed, where a sudden and concurrent change of the group fitness V_∞ [Fig. 4(a)] and consensus χ_∞ [Fig. 4(b)] takes place. For any given value of β', a critical value $(\beta J)_C$ at which the transition from low to high fitness and consensus is completed is identified as the critical threshold of the control parameter βJ. The resulting phase diagram is illustrated in Fig. 4(c), where the solid line

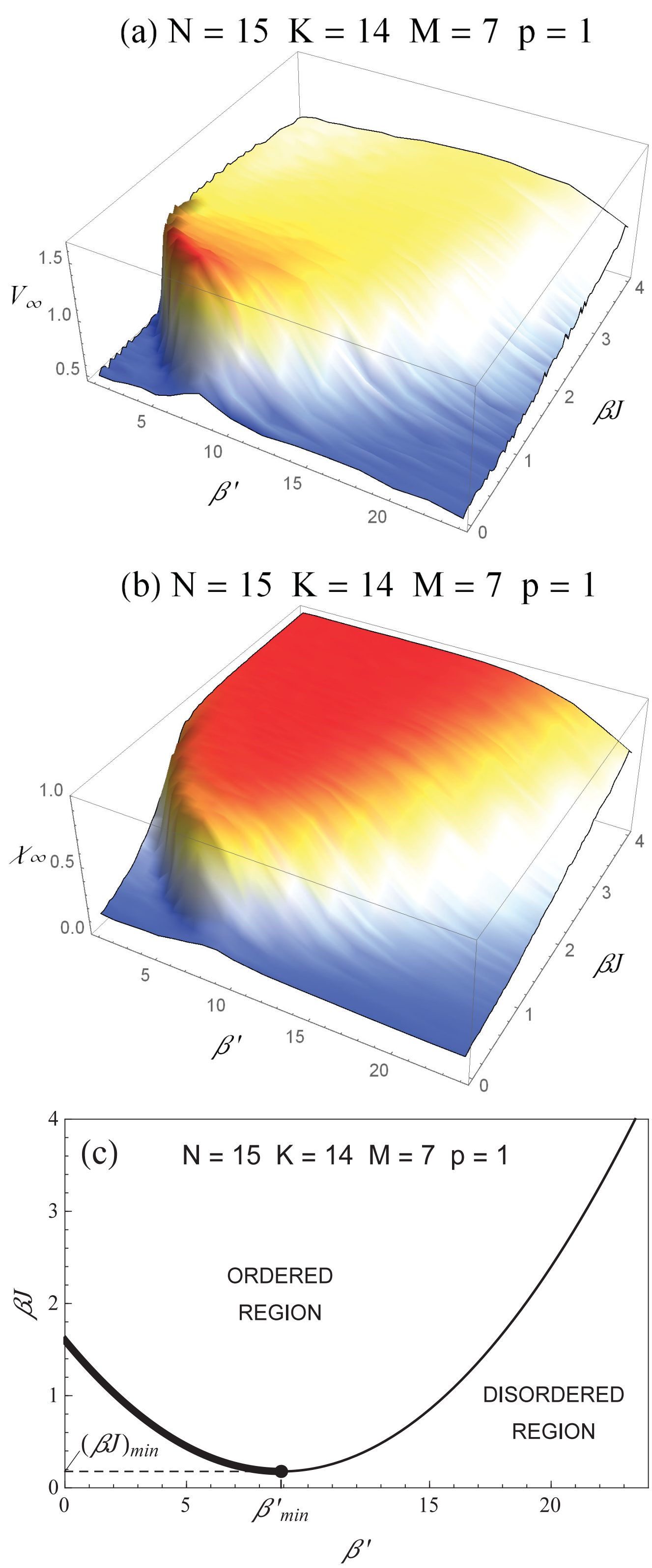

FIG. 4. The stationary values of the normalized averaged fitness V_∞ (a) and of the statistically averaged consensus χ_∞ (b) as a function of βJ and β'. The phase diagram is represented in (c). Results are presented for $p = 1$, $N = 15$, $K = 14$, and $M = 7$.

represents the critical transition front, and two phases can be distinguished: (i) the ordered region where the consensus is high, with the binary opinions (spin) of the agents almost all aligned along the same direction, and (ii) the disordered region where the consensus is low, i.e., where the opinion of the agents are randomly distributed. The critical front comprises a thick branch and a thin one. These two branches are separated by the point of coordinates $\{\beta'_{\rm min},(\beta J)_{\rm min}\}$, where $\beta'_{\rm min}$ is the value of self-confidence β' at which the critical threshold $(\beta J)_C$, needed to complete the transition, takes its minimum value $(\beta J)_{\rm min}$. For $\beta' < \beta'_{\rm min}$ [see Fig. 4(c)], increasing βJ from zero leads to a significantly sharper transition (thick branch). On the other hand, when $\beta' > \beta'_{\rm min}$ a much softer transition occurs (thin branch). Note that for $\beta' = 0$, the only driving force is consensus-seeking. In this case, the system, not being influenced by any information associated with the fitness landscape, follows exactly the Ising-Glauber dynamics, resulting in an inefficient decision-making process in terms of fitness. Increasing the level of self-confidence β' causes the agents to be driven also by self-interest while remaining, for $\beta' < \beta_{\rm min}$, sufficiently prone to changing their mind based on the opinions of the other group members. The presence of the self-interest is then beneficial, since by breaking the symmetry of the pure Ising system, each member is pushed to make choices aimed at increasing the fitness. This in turn also expedites the process of consensus-seeking, decreases the level of social interaction strength needed to trigger the phase transition, and explains why increasing β' from zero makes the critical transition threshold $(\beta J)_C$ decrease down to a minimum value $(\beta J)_{\rm min}$. However, as soon as $\beta' > \beta'_{\rm min}$, agents, because of their high level of self-confidence, are reluctant to change their mind. Thus, even when they are wrong, i.e., even when their choices do not necessarily lead to an increase of fitness, agents hardly accept a changed opinion unless the social interaction strength between them is increased. This leads to higher values of $(\beta J)_C$, to smoother transition, smaller fitness, and, in the end, to a decay in the performance of the group in making decisions.

Increasing the number of agents from $M = 7$ to 21 (see Fig. 5), the overall qualitative trend of the quantities V_∞ and χ_∞ remains almost the same. However, some differences should be noted: (i) for $\beta' < \beta'_{\rm min}$ the fitness V_∞ presents, at the critical transition, a higher peak; (ii) for $\beta' > \beta'_{\rm min}$ the transition is smoother, leading to smaller fitness values; and (iii) the parabola-shaped critical front changes in that $\beta'_{\rm min}$ is significantly decreased and $(\beta J)_{\rm min}$ slightly increased. These changes are clearly shown in Fig. 6, where the critical transition fronts are presented for $M = 7$ (blue line) and $M = 21$ (red line), given $p = 1$, $N = 15$, and $K = 14$. Note the presence of two points: (i) $Q_{\rm min}$ for $M = 7$ and (ii) $P_{\rm min}$ for $M = 21$. These two points identify the minimal values of critical value $(\beta J)_C$ triggering the phase transition. On the thick branch, being $\beta' < \beta'_{\rm min}$, the critical transition is sharp and the step change of group fitness and consensus is very significant. On the thin branch ($\beta' > \beta'_{\rm min}$), the critical transition is smeared and the group-fitness and consensus variations are smaller. Moreover, moving on the thin branch of the front, along the β'-increasing direction, worsens the performance of the decision-making process (see also Figs. 4 and 5).

As mentioned earlier, increasing M makes $\beta'_{\rm min}$ smaller and $(\beta J)_{\rm min}$ slightly larger. This has an important consequence, as, depending on the value of β', increasing the number M of the

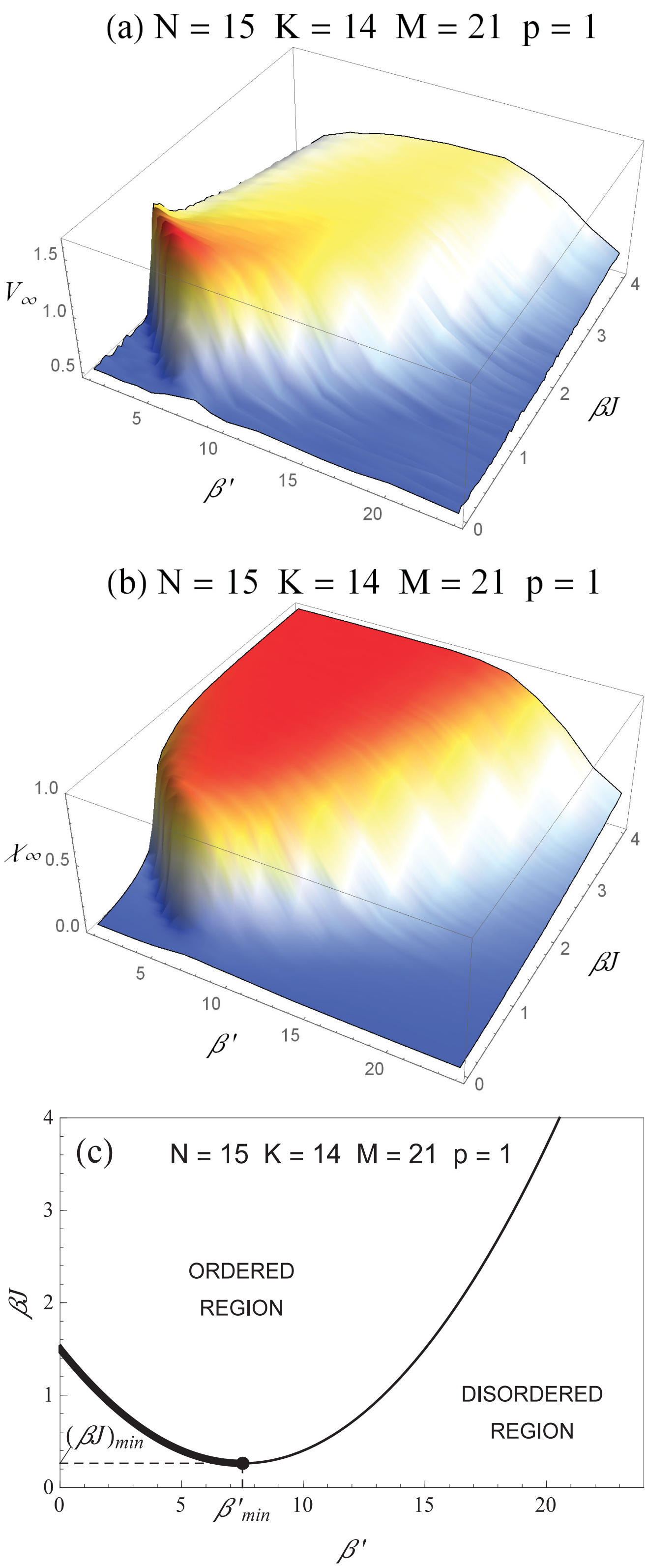

FIG. 5. The stationary values of the normalized averaged fitness V_∞ (a) and of the statistically averaged consensus χ_∞ (b) as a function of βJ and β'. The phase diagram is represented in (c). Results are presented for $p = 1$, $N = 15$, $K = 14$, and $M = 21$.

agents may either be beneficial or detrimental. Indeed, for large β' (i.e., on the thin branch side of the phase diagram in Fig. 6), increasing M worsens the performance of the decision-making process in terms of fitness values. On the other hand, when β' is small (i.e., on the thick branch side of the phase diagram in Fig. 6), increasing M improves the performance of the decision-making process as it leads to an increase of fitness. This makes it clear why in the literature the size of the team is a strongly debated aspect of team design, for some studies show that a small group performs better than big groups, but also the opposite has been demonstrated to occur depending on environmental conditions [78,79].

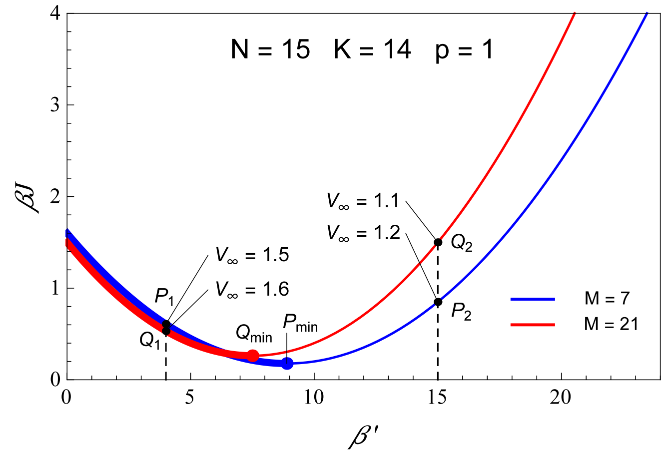

FIG. 6. The critical critical transition fronts for $M = 7$ (blue line) and $M = 21$ (red line). Results are presented for $p = 1$, $N = 15$, and $K = 14$. On the thick part of the lines, the critical transition is sharp and is associated with a very large step from low to high fitness. On the thin line, the critical transition is smeared and the step change in fitness is smaller. It even decreases as one moves along the line to increase β'. Note that increasing M from 7 to 21 makes the point $P_{\min}$ move to $Q_{\min}$, thus $\beta'_{\min}$ decreases significantly whereas $(\beta J)_{\min}$ increases slightly.

So far, we have shown that the collective intelligence of the group (i.e., the ability to make decisions leading to high values of the group fitness) emerges just at the critical transition. The literature [25,63–72] ascribes the emergence of collective intelligence to high values of mutual information and to an increase of information flow among the members of the group. However, in this study we are not interested in determining the level of mutual information among the members of the group, which is a point that has already been sufficiently investigated in the literature. We are interested instead in determining the mutual information between the fitness V_∞ and the consensus χ_∞ within the group. The rationale behind this choice is that the mutual information between fitness and consensus can be considered as a proxy of how much information leaks from the fitness landscape to the group members, and therefore it is an indirect measure of the amount of awareness of the entire group about the fitness landscape itself. The mutual information $\mathrm{MI}(x,y)$ between two stochastically distributed continuous variables x and y is

$$\mathrm{MI}(x,y) = \int dx\, dy\, p(x,y) \log_2 \frac{p(x,y)}{p(x)p(y)}. \qquad (9)$$

It is a measure of the information gained about the behavior of one random variable, say x, by observing the behavior of the other variable y. Hence, the mutual information measures the difference between the initial uncertainty on the variable x and the uncertainty that remains about x after the observation of the behavior of the variable y. From this perspective, it measures the amount of information leakage from the variable y to the variable x, and vice versa.

Figure 7 shows the quantity $\mathrm{MI}(\chi_\infty, V_\infty)$ as a function of the control parameters β' and βJ for $M = 7$ [Fig. 7(a)] and $M = 21$ [Fig. 7(b)]. Results are presented for $p = 1$, $N = 15$, and $K = 14$. Notice that $\mathrm{MI}(\chi_\infty, V_\infty)$ is small everywhere except close to the critical front, where it takes higher values. The highest mutual information is obtained for $\beta' < \beta'_{\mathrm{min}}$, where also the fitness V_∞ and the consensus χ_∞ are maximized. This seems to confirm previous findings, which showed that the mutual information among different spins is maximized at the criticality [65,80]. However, here we go a bit further and find out that also the mutual information between the fitness and the consensus of the group is maximized at the transition threshold. This clearly shows that, at criticality, a significant amount of information leaks from the complex fitness landscape to the group of agents, leading to a superior performance of the group decision making in terms of fitness values. In other words, at the critical threshold, the indirect exchange of information, promoted by social interactions, provides the group with higher knowledge of the fitness landscape. The exploration of the landscape is then strongly improved, leading to better choices and finally to the emergence of the collective intelligence of the group [27].

V. THE EFFECT OF LEVEL OF KNOWLEDGE

The critical dynamics described so far is observed even in the presence of cognitive limits of the agents, i.e., for $p < 1$. Figure 8 show the fitness V_∞ as a function of β' and βJ for $p = 0.3$ [Fig. 8(a)], $p = 0.7$ [Fig. 8(b)], and $p = 1$. [Fig. 8(c)].

The emergence of the collective intelligence, in the presence of the cognitive limits of the agents, can be explained by considering that, at the critical threshold, the agent with limited knowledge will exploit social interactions and consensus-seeking to follow those agents with higher knowledge, resulting in a final consensus about the decisions to make. Note that for $p = 0.7$, the performance of the group, in terms of V_∞ values, is comparable to, although a bit smaller than, $p = 1$ [Fig. 8(c)], whereas if p is sufficiently small, e.g., $p = 0.3$, the performance of the group lowers quite significantly. Figure 9 shows the critical fronts for different values of p. In particular, as p is decreased, a continuous decrease of the minimum value β'_{min} and a concurrent increase of $(\beta J)_{\mathrm{min}}$ can be noted. Thus, as the cognitive capacity of the agents decreases, they need to rely more on the others in order to make good decisions. More importantly, the presence of relatively highly self-confident individuals easily worsens the performance of the group, since self-confident individuals are reluctant to change their mind, thus inhibiting the exploration of the fitness landscape.

VI. THE EFFECT OF LEADERSHIP

It is widely recognized that one of the key features of a charismatic leader is self-confidence. Having a self-confident

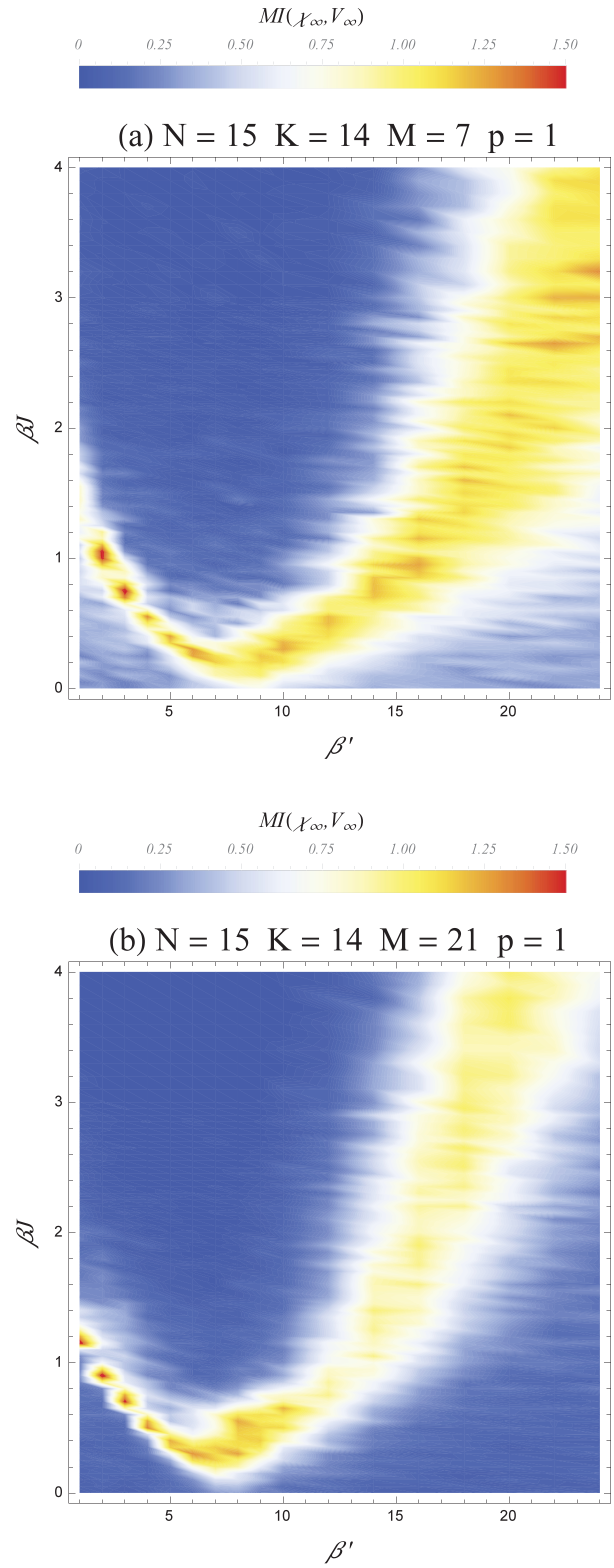

FIG. 7. The mutual information $\mathrm{MI}(\chi_\infty, V_\infty)$, in color scale (blue for low values, red for high values), between the consensus χ_∞ and the group fitness V_∞, $M = 7$ (a) and $M = 21$ (b). Results are presented for $p = 1$, $N = 15$, and $K = 14$. Notice that $\mathrm{MI}(\chi_\infty, V_\infty)$ is small everywhere but close to the critical front, where it takes higher values. The highest mutual information is obtained for $\beta' < \beta'_{\mathrm{min}}$.

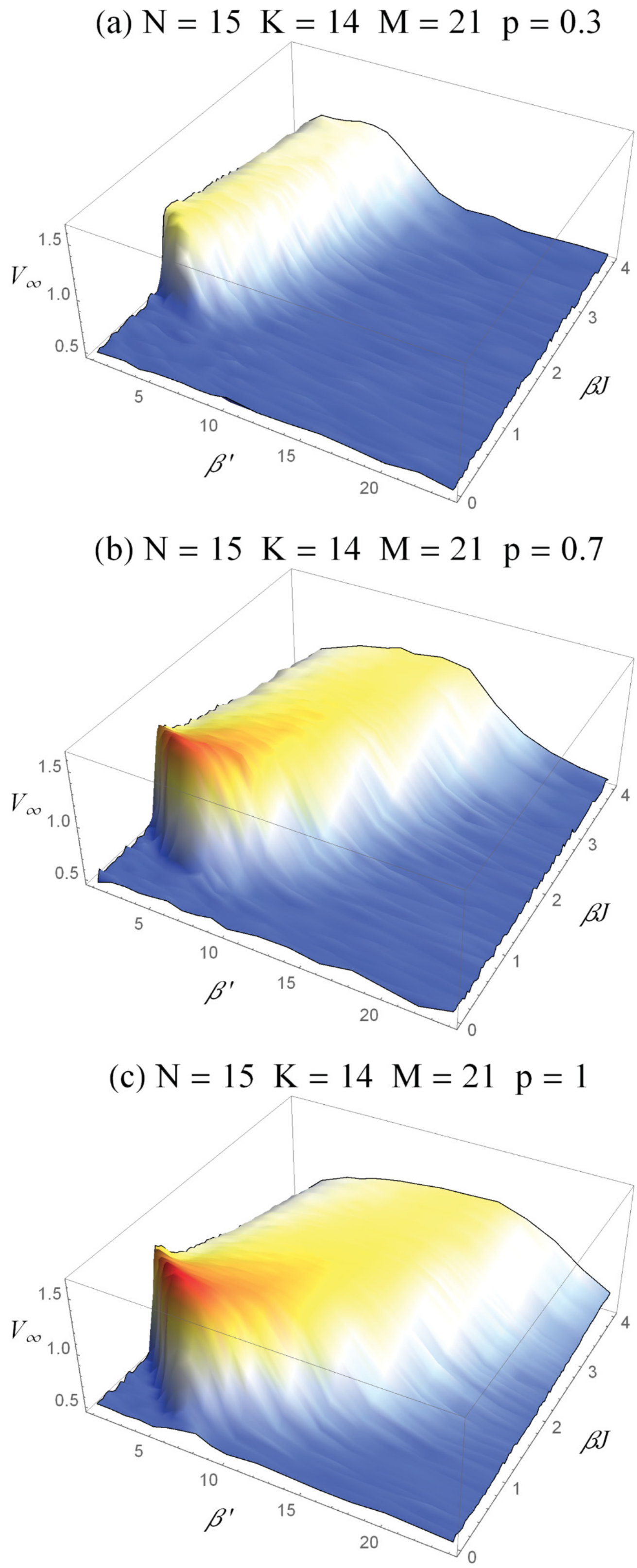

FIG. 8. The stationary values of the normalized averaged fitness V_∞ as a function of βJ and β'. Results are presented for $p = 0.3$ (a), $p = 0.7$ (b), $p = 1$ (c), and for $N = 15$, $K = 14$, and $M = 7$.

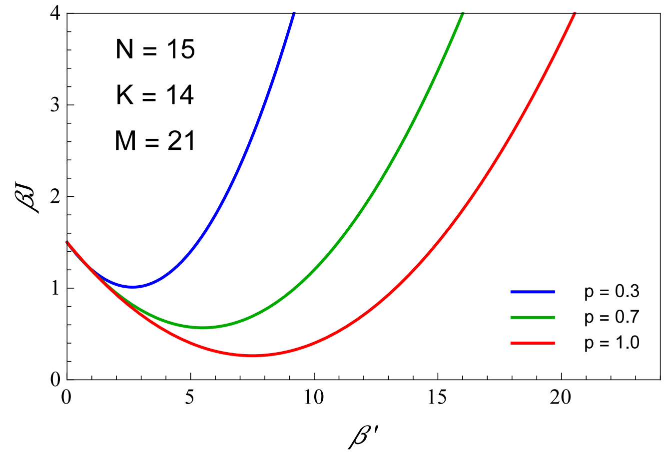

FIG. 9. The critical transition fronts for different levels of knowledge of the agents: $p = 0.3$, 0.7, and 1. Results are presented for $N = 15$, $K = 14$, and $M = 21$. Note that decreasing p reduces $\beta'_{\min}$ and increases $(\beta J)_{\min}$.

leader helps the team to feel the same and pushes it to move ahead and solve problems [81–84]. This type of leadership is nonauthoritative, and it is called participative. Within the proposed model, self-confidence is modeled trough the parameter β'. Therefore, to analyze the effect of the leadership, we assume that the level of confidence of the leader is β'_L, while the other members of the group have smaller confidence, $\beta'_{NL} = \alpha\beta'_L$, where α is a factor ranging in the interval $0 \leqslant \alpha < 1$.

Figure 10 shows the steady-state fitness V_∞ as a function of βJ and α for $M = 7$, $N = 15$, $K = 14$, and $p = 1.0$, and two different levels of confidence of the leader: $\beta'_L = 5$ [Fig. 10(a)] and $\beta'_L = 10$ [Fig. 10(b)]. Figure 10(a) shows that for $\beta'_L < \beta'_{\min}$ (i.e., for a not too confident leader), provided that the system is in the ordered side of the phase diagram but close to the transition front, the best performance is obtained when all members have the same self-confidence as that of the leader. To explain this, let us first consider that, being $\beta'_L < \beta'_{\min}$, the exploration of the landscape is already sufficiently facilitated as agents are prone to change their mind based on the opinion of others. Therefore, values of $\alpha < 1$ would make the agents even more prone to change opinion, and thus to underestimate their self-interest in making decisions. This will make the random walk of the agents on the group fitness landscape too chaotic, hampering an easy identification of the good set of decisions. We conclude that for $\beta'_L < \beta'_{\min}$, the presence of a leader is detrimental. On the other hand, if $\beta'_L > \beta'_{\min}$ [Fig. 10(b)], the fitness of the group is maximized for values of $\alpha < 1$. For $\beta'_L = 10$, i.e., for the specific case considered in Fig. 10(b), results show that the decision-making performance is maximized for $\alpha \approx 0.5$, i.e., when the level of confidence of the leader almost doubles that of the other members. This is evident if one considers that, for $\beta' > \beta_{\min}$, the exploration of the landscape is quite strongly inhibited. But, we have shown that to make a good decision, the exploration of the landscape needs to be enhanced. Lowering the self-confidence β'_{NL} of the other (nonleader) members of the group just makes this happen, leading to better performance. However, if $\beta'_{NL} \ll \beta'_L$, nonleader members will largely neglect their self-interest in making decisions. Thus, driven by consensus-seeking, they

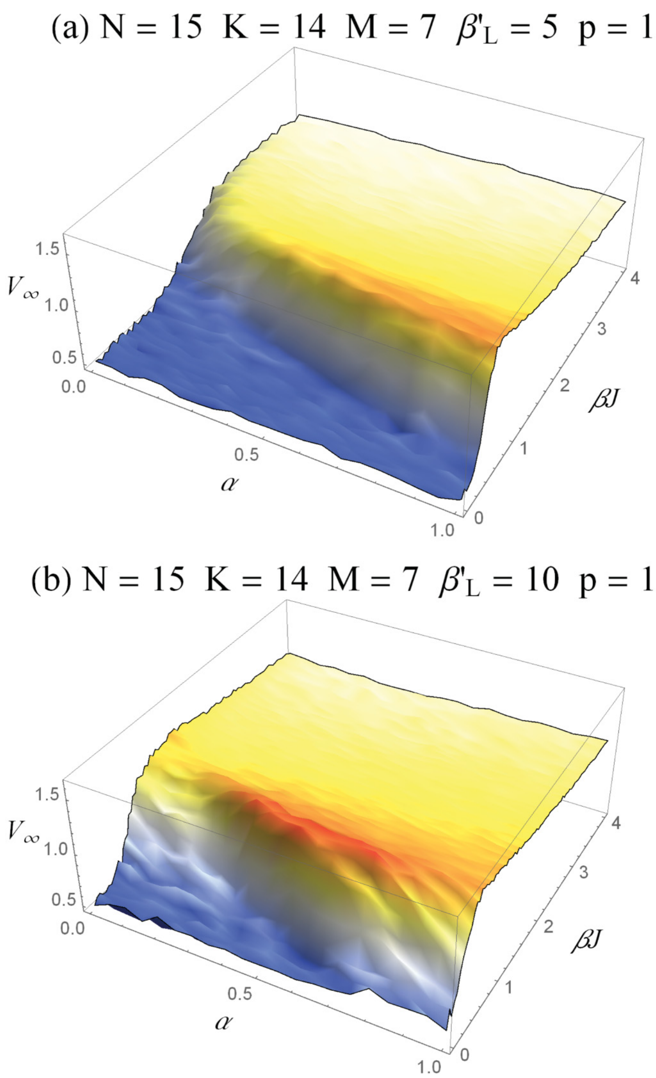

FIG. 10. The stationary values of the normalized averaged fitness V_∞ as a function of βJ and α. Results are presented for $p = 1$, $N = 15$, $K = 14$, $M = 7$, and $\beta'_L = 5$ (a), $\beta'_L = 10$ (b).

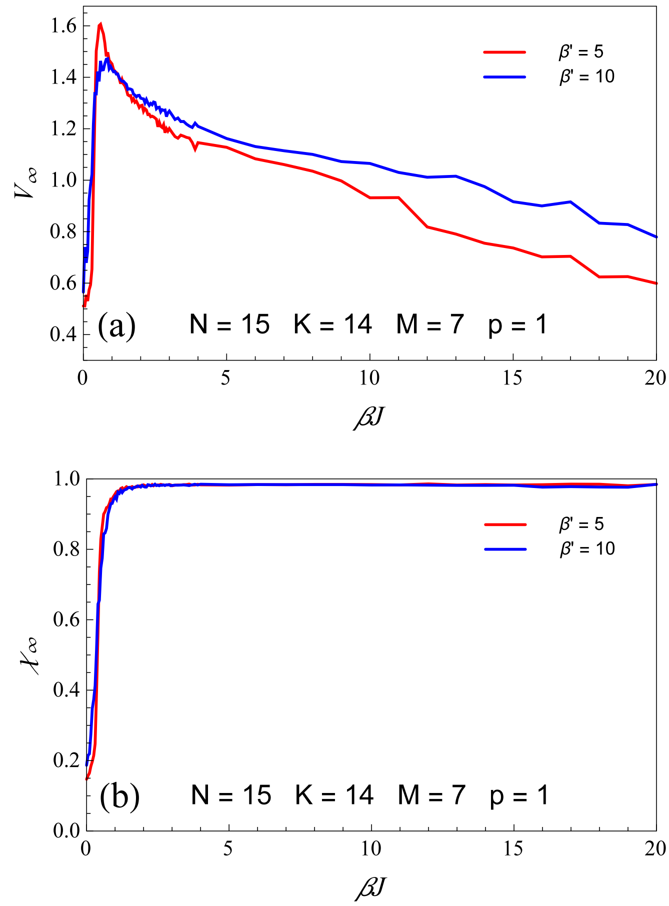

FIG. 11. The occurrence of groupthink. Far from the critical threshold, i.e., for high values of the social interaction strength (high level of trust), the pressure for consensus seeking makes the members completely overlook the effect of their decision on their own perceived fitness. The dynamics of the system resemble the classical dynamics of a pure Ising-like system. This leads to a high value of consensus χ_∞ (b) but to a very low value of group fitness V_∞ (a). Results are presented for $p = 1$, $N = 15$, $K = 14$, $M = 7$, and for $\beta' = 5$ and 10.

will end up following the leader in making decision. But, since the leader already has a high level of self-confidence, the resulting low level of landscape exploration will worsen the performance of the decision-making process.

VII. GROUPTHINK PHENOMENON

In the literature, consensus achievement within groups is often associated with the emergence of collective intelligence [37,38,44]. However, it has also been recognized that consensus-seeking may even lead to a phenomenon known as groupthink [85–87], i.e., a faulty thinking that occurs in highly cohesive groups and leads to an irrational or dysfunctional decision-making outcome. When groupthink occurs, members try to minimize conflict and to reach consensus without critically evaluating possible alternative point of views. Groupthink occurs in situations where members have similar backgrounds, which increases the propensity for them to agree on a rather irrational or poor final decision. Evidence of such a phenomenon emerges naturally in our model as shown in Fig. 11, where V_∞ [Fig. 11(a)] and χ_∞ [Fig. 11(b)] are plotted as a function of βJ for two different values of β'. Indeed, for large values of βJ, i.e., far away from the critical threshold $(\beta J)_C$, the driving force related to consensus-seeking is dominant. This facilitates the achievement of consensus among the members, independent of the level of fitness. The final outcome is simply that the entire group converges to a highly agreed upon but ineffective and inadequate final decision.

VIII. CONCLUSIONS

The present study identifies specific conditions leading to the emergence of collective intelligence in groups of interacting agents. To this purpose, we have employed a recent model of group decision making. This model formulates the decision process of the agents in terms of a time-continuous Markov chain, where the transition rates are defined so as to capture the effect of the self-interest, which pushes each single agent to increase the perceived (individual) fitness, and the social interactions, which stimulate members to seek consensus with the other members of the group. The process is then characterized by three different parameters: (i) the strength of social interaction βJ in units of social temperature β^{-1}, (ii) the level of self-confidence β' of the agents in their own expertise, and (iii) the level of knowledge p of each agent. These parameters all together identify the long-term behavior and the different phases of the system. In particular, critical fronts can be identified at which a concurrent transition from low to high fitness and from low to high consensus within the group takes place. We show that at the critical transition, the mutual information between the fitness landscape and the level of consensus within the group is maximized, demonstrating that, at the criticality, a significant amount of information exchange, promoted by social interactions triggers the emergence of a superior performance of the group in making good decisions, thus leading to the emergence of the collective intelligence of the group. We show that the self-confidence of the agents has an important influence on the performance of the decision-making process. Our simulations show that too high or too low self-confidence levels are deleterious, as they hamper the emergence of collective intelligence. However, for any given size M of the group, an optimal level $\beta'_{\min}$ of self-confidence can be found that minimizes the critical social strength $(\beta J)_C$ required to trigger the transition to the collective intelligent state and to maximize the performance of the group in making decisions. Concerning the effect of M, results show that it can be twofold. In fact, increasing M may lead either to an increase in the performance, if the level of self-confidence of the agents is low, or to a decrease in the performance in the opposite case. We also analyze the effect of the level of knowledge p on the decision-making performance of the group. We show that even at a very low level of knowledge, e.g., $p = 0.3$, the performance of the group can be kept relatively high. However, to this purpose, the agents need to be less self-confident and to trust more in their peers. We also demonstrate that the presence of a highly self-confident leader is not significantly beneficial, and may even be detrimental. Moreover, the social phenomenon of groupthink naturally emerges within the proposed model when the driving force pushing the members toward consensus strongly prevails over the self-confidence level of the agents.

ACKNOWLEDGMENT

The authors warmly thank ARO for support through Grant No. W911NF-15-1-0245.

APPENDIX: THE FITNESS LANDSCAPE

1. The NK model

In the NK model, a real-valued fitness is assigned to each bit string $\mathbf{d} = (d_1, d_2, \ldots, d_N)$, where $d_i = \pm 1$. This is done by first assigning a real-valued contribution W_i to the ith bit d_i, and then by defining the fitness function as $V(\mathbf{d}) = N^{-1} \sum_{i=1}^{N} W_i(d_i, d_1^i, d_2^i, \ldots, d_K^i)$. Each contribution W_i depends not just on i and d_i but also on K ($0 \leqslant K < N - 1$) other bits. Now let us define the substring $\mathbf{s}_i = (d_i, d_1^i, d_2^i, \ldots, d_K^i)$ by choosing at random, for each bit i, K other bits. The number of contributions $W_i(\mathbf{s}_i)$ is equal to the number of different values that can be enumerated with the substring of $k + 1$ binary elements, i.e., it is 2^{K+1}. Each single value $W_i(\mathbf{s}_i)$ is drawn from a uniform distribution, usually in the range $[0,1]$. Thus, a random table of $N \times 2^{K+1}$ contributions is generated independently for each ith bit, allowing the calculation of the fitness function $V(\mathbf{d})$. The reader is referred to Refs. [53,54] for more details on the NK complex landscapes. Notice that increasing the complexity $C = K + 1 + \log_2 N$ not only affects the number of local maxima, but also the autocorrelation of the landscape itself. In particular at the maximum level of complexity, i.e., when $K = N - 1$, one can show that the number of local maxima is $2^N/(N + 1)$ and that the fitness values are completely uncorrelated with each other; in this case, the fitness landscape is represented by an isotropic white noise. This means that when using the NK model, it is not possible to control separately the complexity, the autocorrelation, and the actual level of anisotropy of the landscape. Also, it is worth noting that the stochastic fitness function $V(\mathbf{d})$, being the mean value of several independent uniformly distributed contributions of expectation value $\bar{W} = \langle W \rangle$ and variance $\sigma_W^2 = \langle (W - \bar{W})^2 \rangle$, is very well approximated, as prescribed by the central limit theorem, by a Gaussian distribution with average $\langle V \rangle = \bar{W}$ and variance $\sigma_V^2 = \langle (V - \bar{W})^2 \rangle = \sigma_W^2/N$. Thus, increasing the number of decisions N leads to a decrease of σ_V^2, so that for very large N the distribution of fitness values V degenerates into a Dirac δ distribution centered in $\bar{W}$. To prevent this from occurring, we preferred to rescale the fitness values V in such a way as to keep the same average $\bar{W}$ and the same variance σ_W^2, i.e., we use

$$V \rightarrow \bar{W} + \sqrt{N}\big(V - \bar{W}\big). \tag{A1}$$

2. The spectral method

A different way to generate random landscapes of given complexity is to use spectral methods. The advantage of such methods is that they allow us to control separately the level of complexity, the autocorrelation function, and consequently also the anisotropy of the landscape. We assume that the rugged surface is statistical homogeneous, i.e., translationally invariant. For the sake of simplicity, we also consider that the surface is periodic. Therefore, the rugged surface can be expressed in the form of a Fourier series,

$$h(\mathbf{x}) = \sum_{hk=-\infty}^{+\infty} a_{hk} e^{i \mathbf{q}_{kh} \cdot \mathbf{x}}, \tag{A2}$$

where $\mathbf{x}$ is the in-plane position vector and h is the out-of-plane height of the surface. Also, we have $\mathbf{q}_{kh} = (k,h)$, with $k,h = \ldots,-2,-1,0,1,2,\ldots$ and $\mathbf{x} = (x,y)$. The quantities $a_{hk} = \xi_{kh} + i\eta_{kh}$ satisfy the relation $a_{00} = 0$, $a_{-h,-k} = \overline{a_{hk}}$ to guarantee that $h(\mathbf{x})$ is real, and they are determined by drawing from a Gaussian distribution the random real quantities ξ_{kh} and η_{kh} with zero mean and variance $\langle \xi_{kh}^2 \rangle = \langle \eta_{kh}^2 \rangle = \langle |a_{kh}|^2 \rangle / 2 = \sigma_{hk}^2/2$. One can easily show that $\langle a_{kh} a_{lm} \rangle = \sigma_{kh}^2 \delta_{k,-l} \delta_{h,-m}$, where δ_{ij} is the Kronecker delta operator. Then the autocorrelation function is

$$\langle h(\mathbf{x}')h(\mathbf{x})\rangle = \sum_{kh} \sigma_{kh}^2 e^{i\mathbf{q}_{kh}\cdot(\mathbf{x}'-\mathbf{x})}. \tag{A3}$$

Thus, choosing the quantities σ_{kh}^2 allows us to identify the autocorrelation function of the landscape. Note that the resulting surface $h(\mathbf{x})$ is Gaussian with zero average and variance $\langle h^2\rangle = \sum_{kh}\sigma_{kh}^2$. Now, in order to fully define the rugged landscape $h(\mathbf{x})$, we need to specify the quantities $\mathbf{q}_{kh}$ and σ_{kh}^2. Thus, if we choose an even number $n = 2^{R-1}$, with the integer number $R \geqslant 2$, and if we assume $\mathbf{q}_{kh} = (k,h)$, with $k,h = -n,\ldots,-2,-1,0,1,2,\ldots,n-1$, then we can employ the fast Fourier transform numerical technique to calculate $2n \times 2n = 2^{2R}$ different values h_{ij} of the fitness landscape as

$$h_{ij} = \sum_{hk=-n}^{n-1} a_{hk} e^{i\mathbf{q}_{kh}\cdot\mathbf{x}_{ij}}, \tag{A4}$$

with $\mathbf{x}_{ij} = (\pi i/n,\pi j/n)$, and $i,j = -n,\ldots,-2,-1,0,1,2,\ldots,n-1$. Given the number $N = 2R$, which defined the number of points of the fitness landscape, we can also tune the complexity of the landscape by choosing the number of nonzero coefficients a_{hk}, $h,k = 1,2,\ldots,r$, with $r = 2^L$ (note that $L \leqslant R$). In this case, in order to completely specify the surface, we need to know $r \times r = 2^{2L}$ coefficients a_{hk} plus the single number n so the complexity of the landscape can be estimated as

$$C = \log_2(2^{2L}+1) \approx \log_2 2^{2L} = 2L. \tag{A5}$$

In the case of a fractal-like self-affine surface, the statistical properties of the surface $h(\mathbf{x})$ are invariant under the transformation

$$\mathbf{x} \to t\mathbf{x}, \qquad h \to t^H h, \tag{A6}$$

where the Hurst exponent H is related to the fractal dimension of the surface, $D_f = 3 - H$. For self-affine surfaces, the quantities σ_{hk}^2 satisfy the relation

$$\sigma_{hk}^2 = \sigma_{11}^2 \left(\frac{h^2+k^2}{2}\right)^{-H-1}. \tag{A7}$$

Hence, σ_{hk}^2 can be determined once we know σ_{11}^2 and the fractal dimension of the landscape. The reader is referred to [75] for more details on the generation of a random surface $h(\mathbf{x})$ with spectral techniques.

[1] C. H. Lee and A. Lucas, Phys. Rev. E **90**, 052804 (2014).
[2] C. D. Brummitt, S. Chatterjee, P. S. Dey, and D. Sivakoff, Ann. Appl. Probab. **25**, 2013 (2015).
[3] R. J. G. Clément, S. Krause, N. von Engelhardt, J. J. Faria, J. Krause, and R. H. J. M. Kurvers, PLoS ONE **8**, e77943 (2013).
[4] S. Galam, Physica A **238**, 66 (1997).
[5] S. Galam and A. C. R. Martins, Phys. Rev. E **91**, 012108 (2015).
[6] I. D. Couzin, Trends Cogn. Sci. **13**, 36 (2009).
[7] D. J. T. Sumpter and S. C. Pratt, Philos. Trans. R. Soc. B **364**, 743 (2009).
[8] A. J. W. Ward, D. J. T. Sumpter, I. D. Couzin, P. J. B. Hart, and J. Krause, Proc. Natl. Acad. Sci. USA **105**, 6948 (2008).
[9] S. Arganda, A. Pérez-Escudero, and G. G. de Polavieja, Proc. Natl. Acad. Sci. USA **109**, 20508 (2012).
[10] A. J. W. Ward, J. E. Herbert-Read, D. J. T. Sumpter, and J. Krause, Proc. Natl. Acad. Sci. USA **108**, 2312 (2011).
[11] A. Pérez-Escudero and G. G. de Polavieja, PLoS Comput. Biol. **7**, e1002282 (2011).
[12] D. J. Watts, Proc. Natl. Acad. Sci. USA **99**, 5766 (2002).
[13] M. Turalska, M. Lukovic, B. J. West, and P. Grigolini, Phys. Rev. E **80**, 021110 (2009).
[14] Z. Wang, A. Szolnoki, and M. Perc, Sci. Rep. **3**, 2470 (2013).
[15] Z. Wang, A. Szolnoki, and M. Perc, Sci. Rep. **3**, 1183 (2013).
[16] G. Koraimann and M. A. Wagner, Front. Cell. Infect. Microbiol. **4**, 54 (2014).
[17] R. Popat, S. A. Crusz, and S. P. Diggle, Br. Med. Bull. **87**, 63 (2008).
[18] H. V. Westerhoff, A. N. Brooks, E. Simeonidis *et al.*, Front. Microbiol. **5**, 379 (2014).
[19] M. J. B. Krieger, J.-B. Billeter, and L. Keller, Nature (London) **406**, 992 (2000).
[20] M. Rubenstein, A. Cornejo, and R. Nagpal, Science **345**, 795 (2014).
[21] J. Werfel, K. Petersen, and R. Nagpal, Science **343**, 754 (2014).
[22] M. Brambilla, E. Ferrante, M. Birattari, and M. Dorigo, Swarm Intell. **7**, 1 (2013).
[23] E. Bonabeau, M. Dorigo, and G. Theraulaz, Nature (London) **406**, 39 (2000).
[24] S. Garnier, J. Gautrais, and G. Theraulaz, Swarm Intell. **1**, 3 (2007).
[25] F. Vanni, M. Luković, and P. Grigolini, Phys. Rev. Lett. **107**, 078103 (2011).
[26] D. Easley and J. Kleinberg, *Networks, Crowds, and Markets: Reasoning about a Highly Connected World* (Cambridge University Press, Cambridge, 2010).
[27] A. Williams Woolley, C. F. Chabris, A. Pentland, N. Hashmi, and T. W. Malone, Science **330**, 686 (2010).
[28] D. Engel, A. W. Woolley, L. X. Jing, C. F. Chabris, and T. W. Malone, PLoS ONE **9**, e115212 (2014).
[29] T. Vicsek and A. Zafeiris, Phys. Rep. **517**, 71 (2012).
[30] L. Conradt and T. J. Roper, Nature (London) **421**, 155 (2003).
[31] I. D. Couzin, J. Krause, N. R. Franks, and S. A. Levin, Nature (London) **433**, 513 (2005).
[32] D. J. G. Pearce and L. Giomi, Phys. Rev. E **94**, 022612 (2016).
[33] M. I. Rabinovich, R. Huerta, and V. Afraimovich, Phys. Rev. Lett. **97**, 188103 (2006).
[34] C. Borghesi, L. Hernández, R. Louf, and F. Caparros, Phys. Rev. E **88**, 062813 (2013).
[35] A. Lucas and C. H. Lee, Phys. Rev. E **87**, 032806 (2013).
[36] É. Roldán, I. Neri, M. Dörpinghaus, H. Meyr, and F. Jülicher, Phys. Rev. Lett. **115**, 250602 (2015).
[37] I. D. Couzin, C. C. Ioannou, G. Demirel, T. Gross, C. J. Torney, A. Hartnett, and N. E. Leonard, Science **334**, 1578 (2011).
[38] A. T. Hartnett, E. Schertzer, S. A. Levin, and I. D. Couzin, Phys. Rev. Lett. **116**, 038701 (2016).

[39] A. B. Kao and I. D. Couzin, Proc. R. Soc. B **281**, 20133305 (2014).
[40] W. Oh and S. Jeon, Manage. Sci. **53**, 1086 (2007).
[41] M. Moussaïd, J. E. Kämmer, P. P. Analytis, and H. Neth, PloS One **8**, e78433 (2013).
[42] L. Muchnik, S. Aral, and S. J. Taylor, Science **341**, 647 (2013).
[43] A. Mani, I. Rahwan, and A. Pentland, Sci. Rep. **3**, 1735 (2013).
[44] L. Rendell, R. Boyd, D. Cownden, M. Enquist, K. Eriksson, M. W. Feldman, L. Fogarty, S. Ghirlanda, T. Lillicrap, and K. N. Laland, Science **328**, 208 (2010).
[45] P. J. DiMaggio and W. W. Powell, Am. Soc. Rev. **48**, 147 (1983).
[46] S. Galam, Y. Gefen, and Y. Shapir, J. Math. Soc. **9**, 1 (1982).
[47] L. Pareschi, P. Vellucci, and M. Zanella, Physica A **467**, 201 (2017).
[48] K. Mahmoodi and P. Grigolini, J. Phys. A **50**, 015101 (2016).
[49] M. Turalska and B. J. West, Phys. Rev. E **90**, 052815 (2014).
[50] G. Carbone and I. Giannoccaro, Eur. Phys. J. B **88**, 339 (2015).
[51] C. Castellano, S. Fortunato, and V. Loreto, Rev. Mod. Phys. **81**, 591 (2009).
[52] R. J. Glauber, J. Math. Phys. **4**, 294 (1963).
[53] S. Kauffman and S. Levin, J. Theor. Biol. **128**, 11 (1987).
[54] S. Kauffman and E. Weinberger, J. Theor. Biol. **141**, 211 (1989).
[55] D. Sornette, Rep. Prog. Phys. **77**, 062001 (2014).
[56] W. Weidlich, Br. J. Math. Stat. Psychol. **24**, 251 (1971).
[57] E. Ising, Z. Phys. **31**, 253 (1925).
[58] S. G. Brush, Rev. Mod. Phys. **39**, 883 (1967).
[59] W. Weidlich, Phys. Rep. **204**, 1 (1991).
[60] F. Schweitzer, *Springer Series in Synergetics—Springer Complexity* (Springer, Berlin, 2007).
[61] D. T. Gillespie, J. Comput. Phys. **22**, 403 (1976).
[62] D. T. Gillespie, J. Phys. Chem. **81**, 2340 (1977).
[63] P. Grigolini, N. Piccinini, A. Svenkeson, P. Pramukkul, D. Lambert, and B. J. West, Front. Bioeng. Biotechnol. **3**, 78 (2015).
[64] M. Turalska, E. Geneston, B. J. West, P. Allegrini, and P. Grigolini, Front. Physiol. **3**, 52 (2012).
[65] R. Guevara Erra, D. M. Mateos, R. Wennberg, and J. L. Perez Velazquez, Phys. Rev. E **94**, 052402 (2016).
[66] L. Barnett, J. T. Lizier, M. Harré, A. K. Seth, and T. Bossomaier, Phys. Rev. Lett. **111**, 177203 (2013).
[67] O. Kinouchi and M. Copelli, Nat. Phys. **2**, 348 (2006).
[68] T. Mora and W. Bialek, J. Stat. Phys. **144**, 268 (2011).
[69] M. Luković, F. Vanni, A. Svenkeson, and P. Grigolini, Physica A **416**, 430 (2014).
[70] R. T. Wicks, S. C. Chapman, and R. O. Dendy, Phys. Rev. E **75**, 051125 (2007).
[71] A. S. Ribeiro, S. A. Kauffman, J. Lloyd-Price, B. Samuelsson, and J. E. S. Socolar, Phys. Rev. E **77**, 011901 (2008).
[72] M. Turalska, B. J. West, and P. Grigolini, Phys. Rev. E **83**, 061142 (2011).
[73] D. L. Applegate, R. M. Bixby, V. Chvátal, and W. J. Cook, *The Traveling Salesman Problem: A Computational Study* (Princeton University Press, Princeton, NJ, 2006).
[74] G. B. Mathews, Proc. London Math. Soc. **s1-28**, 486 (1896).
[75] B. N. J. Persson, O. Albohr, U. Tartaglino, A. I. Volokitin, and E. Tosatti, J. Phys.: Condens. Matter. **17**, R1 (2005).
[76] M. R. Garey and D. S. Johnson, *Computers and Intractability: A Guide to the Theory of NP–Completeness* (Freeman, New York, 1979).
[77] E. D. Weinberger, Santa Fe Institute working paper: 1996-02-003, http://www.santafe.edu/media/workingpapers/96-02-003.pdf (1996).
[78] A. Mao, W. Mason, S. Suri, and D. J. Watts, PloS One **11**, e0153048 (2016).
[79] J. Lorenz, H. Rauhut, F. Schweitzer, and D. Helbing, Proc. Natl. Acad. Sci. USA **108**, 9020 (2011).
[80] H. Matsuda, K. Kudo, R. Nakamura *et al.*, Int. J. Theor. Phys. **35**, 839 (1996).
[81] G. E. Prussia, J. S. Anderson, and C. C. Manz, J. Organiz. Behav. **19**, 523 (1998).
[82] D. Kipnis and W. P. Lane, J. Appl. Psych. **46**, 291 (1962).
[83] M. J. McCormick, J. Leadership Organiz. Stud. **8**, 22 (2016).
[84] G. Yukl, *Leadership in Organizations* (Pearson Education Limited, Edinburgh, 2013).
[85] J. S. Russell, J. Hawthorne, and L. Buchak, Philos. Stud. **172**, 1287 (2015).
[86] C. Mayo-Wilson, K. Zollman, and D. Danks, Int. J. Game Theor. **42**, 695 (2013).
[87] M. Solomon, South. J. Philos. **44**, 28 (2006).